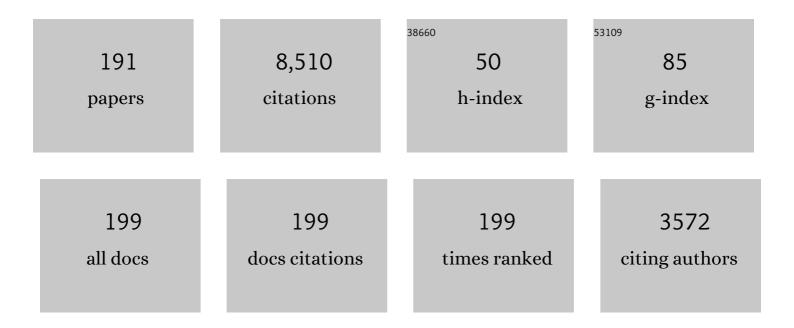
List of Publications by Year in descending order

Source: https://exaly.com/author-pdf/5555100/publications.pdf Version: 2024-02-01



#	Article	IF	CITATIONS
1	Laser-induced incandescence: recent trends and current questions. Applied Physics B: Lasers and Optics, 2006, 83, 333-354.	1.1	427
2	The chemical effects of carbon dioxide as an additive in an ethylene diffusion flame: implications for soot and NOx formation. Combustion and Flame, 2001, 125, 778-787.	2.8	341
3	Laser-induced incandescence: Particulate diagnostics for combustion, atmospheric, and industrial applications. Progress in Energy and Combustion Science, 2015, 51, 2-48.	15.8	295
4	The chemical effect of CO2 replacement of N2 in air on the burning velocity of CH4 and H2 premixed flames. Combustion and Flame, 2003, 133, 495-497.	2.8	283
5	Determination of the soot absorption function and thermal accommodation coefficient using low-fluence LII in a laminar coflow ethylene diffusion flame. Combustion and Flame, 2004, 136, 180-190.	2.8	236
6	Spectrally Resolved Measurement of Flame Radiation to Determine Soot Temperature and Concentration. AIAA Journal, 2002, 40, 1789-1795.	1.5	234
7	A calibration-independent laser-induced incandescence technique for soot measurement by detecting absolute light intensity. Applied Optics, 2005, 44, 6773.	2.1	209
8	The effect of hydrogen addition on flammability limit and NOx emission in ultra-lean counterflow CH4/air premixed flames. Proceedings of the Combustion Institute, 2005, 30, 303-311.	2.4	185
9	Soot concentration and temperature measurements in co-annular, nonpremixed CH/air laminar flames at pressures up to 4 MPa. Combustion and Flame, 2005, 140, 222-232.	2.8	168
10	Two-dimensional imaging of soot volume fraction in laminar diffusion flames. Applied Optics, 1999, 38, 2478.	2.1	164
11	Numerical study on the influence of hydrogen addition on soot formation in a laminar ethylene–air diffusion flame. Combustion and Flame, 2006, 145, 324-338.	2.8	156
12	Heat conduction from a spherical nano-particle: status of modeling heat conduction in laser-induced incandescence. Applied Physics B: Lasers and Optics, 2006, 83, 355-382.	1.1	134
13	Effects of gas and soot radiation on soot formation in a coflow laminar ethylene diffusion flame. Journal of Quantitative Spectroscopy and Radiative Transfer, 2002, 73, 409-421.	1.1	127
14	Deconvolution of axisymmetric flame properties using Tikhonov regularization. Applied Optics, 2006, 45, 4638.	2.1	126
15	Flame front surface characteristics in turbulent premixed propane/air combustion. Combustion and Flame, 2000, 120, 407-416.	2.8	112
16	Inner cutoff scale of flame surface wrinkling in turbulent premixed flames. Combustion and Flame, 1995, 103, 107-114.	2.8	111
17	Modeling of soot aggregate formation and size distribution in a laminar ethylene/air coflow diffusion flame with detailed PAH chemistry and an advanced sectional aerosol dynamics model. Proceedings of the Combustion Institute, 2009, 32, 761-768.	2.4	109
18	Numerical modelling of soot formation and oxidation in laminar coflow non-smoking and smoking ethylene diffusion flames. Combustion Theory and Modelling, 2003, 7, 301-315.	1.0	106

#	Article	IF	CITATIONS
19	Effects of radiation model on the modeling of a laminar coflow methane/air diffusion flame. Combustion and Flame, 2004, 138, 136-154.	2.8	103
20	Influence of polydisperse distributions of both primary particle and aggregate size on soot temperature in low-fluence LII. Applied Physics B: Lasers and Optics, 2006, 83, 383-395.	1.1	100
21	Characterization of flame front surfaces in turbulent premixed methane/Air combustion. Combustion and Flame, 1995, 101, 461-470.	2.8	99
22	Numerical and experimental study of an axisymmetric coflow laminar methane–air diffusion flame at pressures between 5 and 40 atmospheres. Combustion and Flame, 2006, 146, 456-471.	2.8	96
23	Review of recent literature on the light absorption properties of black carbon: Refractive index, mass absorption cross section, and absorption function. Aerosol Science and Technology, 2020, 54, 33-51.	1.5	96
24	Investigation of optical properties of aging soot. Applied Physics B: Lasers and Optics, 2011, 104, 273-283.	1.1	95
25	Application of the statistical narrow-band correlated-k method to low-resolution spectral intensity and radiative heat transfer calculations — effects of the quadrature scheme. International Journal of Heat and Mass Transfer, 2000, 43, 3119-3135.	2.5	94
26	Effects of primary soot particle size distribution on the temperature of soot particles heated by a nanosecond pulsed laser in an atmospheric laminar diffusion flame. International Journal of Heat and Mass Transfer, 2006, 49, 777-788.	2.5	91
27	Are Emissions of Black Carbon from Gasoline Vehicles Underestimated? Insights from Near and On-Road Measurements. Environmental Science & Technology, 2012, 46, 4819-4828.	4.6	91
28	Clouds Over Soot Evaporation: Errors in Modeling Laser-Induced Incandescence of Soot. Journal of Heat Transfer, 2001, 123, 814-818.	1.2	90
29	ls vaccination against hepatitis B infection indicated in patients waiting for or after orthotopic liver transplantation?. Liver Transplantation, 1998, 4, 128-132.	1.9	89
30	An experimental and numerical study of the effects of dimethyl ether addition to fuel on polycyclic aromatic hydrocarbon and soot formation in laminar coflow ethylene/air diffusion flames. Combustion and Flame, 2011, 158, 547-563.	2.8	89
31	The flame preheating effect on numerical modelling of soot formation in a two-dimensional laminar ethylene–air diffusion flame. Combustion Theory and Modelling, 2002, 6, 173-187.	1.0	82
32	Measurement of Aircraft Engine Non-Volatile PM Emissions: Results of the Aviation-Particle Regulatory Instrumentation Demonstration Experiment (A-PRIDE) 4 Campaign. Aerosol Science and Technology, 2015, 49, 472-484.	1.5	82
33	Diffuse-light two-dimensional line-of-sight attenuation for soot concentration measurements. Applied Optics, 2008, 47, 694.	2.1	80
34	Sooting turbulent jet flame: characterization andÂquantitativeÂsootÂmeasurements. Applied Physics B: Lasers and Optics, 2011, 104, 409-425.	1.1	77
35	Radiation heat transfer in planar SOFC electrolytes. Journal of Power Sources, 2006, 157, 302-310.	4.0	76
36	Determination of the morphology of soot aggregates using the relative optical density method for the analysis of TEM images. Combustion and Flame, 2006, 144, 782-791.	2.8	74

#	Article	IF	CITATIONS
37	Application of the statistical narrow-band correlated-k method to non-grey gas radiation in CO2–H2O mixtures: approximate treatments of overlapping bands. Journal of Quantitative Spectroscopy and Radiative Transfer, 2001, 68, 401-417.	1.1	69
38	A Numerical Study on the Influence of CO ₂ Addition on Soot Formation in an Ethylene/Air Diffusion Flame. Combustion Science and Technology, 2008, 180, 1695-1708.	1.2	68
39	Evaluation and Comparison of Portable Emissions Measurement Systems and Federal Reference Methods for Emissions from a Back-Up Generator and a Diesel Truck Operated on a Chassis Dynamometer. Environmental Science & Technology, 2007, 41, 6199-6204.	4.6	67
40	Distribution of the number of primary particles of soot aggregates in a nonpremixed laminar flame. Combustion and Flame, 2004, 138, 195-198.	2.8	66
41	A numerical study of soot aggregate formation in a laminar coflow diffusion flame. Combustion and Flame, 2009, 156, 697-705.	2.8	65
42	Comparison of LII derived soot temperature measurements withÂLII model predictions forÂsoot in aÂlaminar diffusion flame. Applied Physics B: Lasers and Optics, 2009, 96, 657-669.	1.1	63
43	Determination of PM mass emissions from an aircraft turbine engine using particle effective density. Atmospheric Environment, 2014, 99, 500-507.	1.9	59
44	Effects of primary particle diameter and aggregate size distribution on the temperature of soot particles heated by pulsed lasers. Journal of Quantitative Spectroscopy and Radiative Transfer, 2005, 93, 301-312.	1.1	58
45	Laser induced incandescence measurements of soot volume fraction and effective particle size in a laminar co-annular non-premixed methane/air flame at pressures between 0.5–4.0ÂMPa. Applied Physics B: Lasers and Optics, 2006, 83, 469-475.	1.1	58
46	Sensitivity and relative error analyses of soot temperature andÂvolume fraction determined by two-color LII. Applied Physics B: Lasers and Optics, 2009, 96, 623-636.	1.1	57
47	Time-resolved measurements of black carbon light absorption enhancement in urban and near-urban locations of southern Ontario, Canada. Atmospheric Chemistry and Physics, 2011, 11, 10407-10432.	1.9	57
48	Non-grey gas radiative transfer analyses using the statistical narrow-band model. International Journal of Heat and Mass Transfer, 1998, 41, 2227-2236.	2.5	55
49	Soot temperature and volume fraction retrieval from spectrally resolved flame emission measurement in laminar axisymmetric coflow diffusion flames: Effect of self-absorption. Combustion and Flame, 2013, 160, 1693-1705.	2.8	54
50	Band Lumping Strategy for Radiation Heat Transfer Calculations Using a Narrowband Model. Journal of Thermophysics and Heat Transfer, 2000, 14, 278-281.	0.9	53
51	Determining aerosol particle size distributions using time-resolved laser-induced incandescence. Applied Physics B: Lasers and Optics, 2007, 87, 363-372.	1.1	53
52	Precision of multiplex CARS temperatures using both single-mode and multimode pump lasers. Applied Optics, 1987, 26, 99.	2.1	51
53	An efficient approach for the implementation of the SNB based correlated-k method and its evaluation. Journal of Quantitative Spectroscopy and Radiative Transfer, 2004, 84, 465-475.	1.1	51
54	Investigation of Absorption and Scattering Properties of Soot Aggregates of Different Fractal Dimension at 532Ânm Using RDG and GMM. Aerosol Science and Technology, 2013, 47, 1393-1405.	1.5	51

#	Article	IF	CITATIONS
55	Raman spectroscopy and TEM characterization of solid particulate matter emitted from soot generators and aircraft turbine engines. Aerosol Science and Technology, 2017, 51, 518-531.	1.5	51
56	Implementation of an advanced fixed sectional aerosol dynamics model with soot aggregate formation in a laminar methane/air coflow diffusion flame. Combustion Theory and Modelling, 2008, 12, 621-641.	1.0	50
57	Effects of gas and soot radiation on soot formation in counterflow ethylene diffusion flames. Journal of Quantitative Spectroscopy and Radiative Transfer, 2004, 84, 501-511.	1.1	49
58	Effect of aggregation on the absorption cross-section of fractal soot aggregates and its impact on LII modelling. Journal of Quantitative Spectroscopy and Radiative Transfer, 2010, 111, 302-308.	1.1	49
59	Effect of Drive Cycle and Gasoline Particulate Filter on the Size and Morphology of Soot Particles Emitted from a Gasoline-Direct-Injection Vehicle. Environmental Science & Technology, 2015, 49, 11950-11958.	4.6	48
60	Development of absolute intensity multi-angle light scattering for the determination of polydisperse soot aggregate properties. Proceedings of the Combustion Institute, 2011, 33, 847-854.	2.4	47
61	Soot formation in a laminar ethylene/air diffusion flame at pressures from 1 to 8 atm. Proceedings of the Combustion Institute, 2013, 34, 1795-1802.	2.4	47
62	Asymptotic analysis of radiative extinction in counterflow diffusion flames of nonunity Lewis numbers. Combustion and Flame, 2000, 121, 275-287.	2.8	46
63	A numerical and experimental study of a laminar sooting coflow Jet-A1 diffusion flame. Proceedings of the Combustion Institute, 2011, 33, 601-608.	2.4	45
64	Surface density measurements of turbulent premixed flames in a spark-ignition engine and a bunsen-type burner using planar laser-induced fluorescence. Proceedings of the Combustion Institute, 1996, 26, 427-435.	0.3	44
65	Soot and NO formation in counterflow ethylene/oxygen/nitrogen diffusion flames. Combustion Theory and Modelling, 2004, 8, 475-489.	1.0	42
66	Numerical study of the superadiabatic flame temperature phenomenon in hydrocarbon premixed flames. Proceedings of the Combustion Institute, 2002, 29, 1543-1550.	2.4	41
67	Investigation of Thermal Accommodation Coefficients in Time-Resolved Laser-Induced Incandescence. Journal of Heat Transfer, 2008, 130, .	1.2	40
68	Molecular dynamics simulations of translational thermal accommodation coefficients for time-resolved LII. Applied Physics B: Lasers and Optics, 2009, 94, 39-49.	1.1	40
69	FLAME SURFACE DENSITIES IN PREMIXED COMBUSTION AT MEDIUM TO HIGH TURBULENCE INTENSITIES. Combustion Science and Technology, 2007, 179, 191-206.	1.2	39
70	Measurement and modeling of the sooting propensity of binary fuel mixtures. Proceedings of the Combustion Institute, 2007, 31, 611-619.	2.4	38
71	Combination of LII and extinction measurements for determination of soot volume fraction and estimation of soot maturity in non-premixed laminar flames. Applied Physics B: Lasers and Optics, 2015, 119, 685-696.	1.1	38
72	A Numerical Investigation of Thermal Diffusion Influence on Soot Formation in Ethylene/Air Diffusion Flames. International Journal of Computational Fluid Dynamics, 2004, 18, 139-151.	0.5	35

#	Article	IF	CITATIONS
73	On the effect of carbon monoxide addition on soot formation in a laminar ethylene/air coflow diffusion flame. Combustion and Flame, 2009, 156, 1135-1142.	2.8	35
74	Particle Emission Characteristics of a Gas Turbine with a Double Annular Combustor. Aerosol Science and Technology, 2015, 49, 842-855.	1.5	35
75	Modeling of Oxidation-Driven Soot Aggregate Fragmentation in a Laminar Coflow Diffusion Flame. Combustion Science and Technology, 2010, 182, 491-504.	1.2	34
76	Equivalence ratio gradient effects on flame front topology in a stratified iso-octane/air turbulent V-flame. Proceedings of the Combustion Institute, 2011, 33, 1551-1558.	2.4	33
77	Measurement of soot morphology by integrated LII and elastic light scattering. Applied Physics B: Lasers and Optics, 2011, 104, 385-397.	1.1	32
78	A numerical study on NOx formation in laminar counterflow CH4/air triple flames. Combustion and Flame, 2005, 143, 282-298.	2.8	31
79	An Improved Soot Formation Model for 3D Diesel Engine Simulations. Journal of Engineering for Gas Turbines and Power, 2007, 129, 877-884.	0.5	31
80	Determination of the soot aggregate size distribution from elastic light scattering through Bayesian inference. Journal of Quantitative Spectroscopy and Radiative Transfer, 2011, 112, 1099-1107.	1.1	31
81	Effective Density and Mass-Mobility Exponent of Aircraft Turbine Particulate Matter. Journal of Propulsion and Power, 2015, 31, 573-582.	1.3	31
82	Numerical investigation of the effect of signal trapping on soot measurements using LII in laminar coflow diffusion flames. Applied Physics B: Lasers and Optics, 2009, 96, 671-682.	1.1	30
83	Size and shape distributions of carbon black aggregates by transmission electron microscopy. Carbon, 2018, 130, 822-833.	5.4	30
84	Characterization of particulate matter emitted by a marine engine operated with liquefied natural gas and diesel fuels. Atmospheric Environment, 2020, 220, 117030.	1.9	30
85	A novel miniature inverted-flame burner for the generation of soot nanoparticles. Aerosol Science and Technology, 2019, 53, 184-195.	1.5	29
86	Comparison of standardized sampling and measurement reference systems for aircraft engine non-volatile particulate matter emissions. Journal of Aerosol Science, 2020, 145, 105557.	1.8	29
87	The effect of particle aggregation on the absorption and emission properties of mono- and polydisperse soot aggregates. Applied Physics B: Lasers and Optics, 2011, 104, 343-355.	1.1	28
88	Modeling DME Addition Effects to Fuel on PAH and Soot in Laminar Coflow Ethylene/Air Diffusion Flames Using Two PAH Mechanisms. Combustion Science and Technology, 2012, 184, 966-979.	1.2	28
89	In-Situ Real-Time Characterization of Particulate Emissions from a Diesel Engine Exhaust by Laser-Induced Incandescence. , 2000, , .		26
90	The interaction between soot and NO formation in a laminar axisymmetric coflow ethylene/air diffusion flame. Combustion and Flame, 2007, 149, 225-233.	2.8	26

#	Article	IF	CITATIONS
91	Methodology for quantifying the volatile mixing state of an aerosol. Aerosol Science and Technology, 2016, 50, 759-772.	1.5	26
92	Effective density and volatility of particles sampled from a helicopter gas turbine engine. Aerosol Science and Technology, 2017, 51, 704-714.	1.5	26
93	The effect of reformate gas enrichment on extinction limits and NOX formation in counterflow CH4/air premixed flames. Proceedings of the Combustion Institute, 2007, 31, 1197-1204.	2.4	25
94	Characterization of black carbon particles generated by a propane-fueled miniature inverted soot generator. Journal of Aerosol Science, 2019, 135, 46-57.	1.8	25
95	Particulate Matter Measurements in a Diesel Engine Exhaust by Laser-Induced Incandescence and the Standard Gravimetric Procedure. , 0, , .		24
96	A review on the morphological properties of non-volatile particulate matter emissions from aircraft turbine engines. Journal of Aerosol Science, 2020, 139, 105467.	1.8	24
97	Concurrent Quantitative Laser-Induced Incandescence and SMPS Measurements of EGR Effects on Particulate Emissions from a TDI Diesel Engine. , 0, , .		23
98	Heat release rate variations in a globally stoichiometric, stratified iso-octane/air turbulent V-flame. Combustion and Flame, 2015, 162, 944-959.	2.8	23
99	Measurement of soot volume fraction and primary particle diameter in oxygen enriched ethylene diffusion flames using the laser-induced incandescence technique. Energy, 2019, 177, 421-432.	4.5	23
100	Effect of detector nonlinearity and image persistence on CARS derived temperatures. Applied Optics, 1989, 28, 3233.	2.1	22
101	Nonlinearity and image persistence of P-20 phosphor-based intensified photodiode array detectors used in CARS spectroscopy. Applied Optics, 1989, 28, 3226.	2.1	21
102	Effects of soot absorption and scattering on LII intensities in laminar coflow diffusion flames. Journal of Quantitative Spectroscopy and Radiative Transfer, 2008, 109, 337-348.	1.1	21
103	Radiative Properties of Numerically Generated Fractal Soot Aggregates: The Importance of Configuration Averaging. Journal of Heat Transfer, 2010, 132, .	1.2	21
104	Laser-induced incandescence for non-soot nanoparticles: recent trends and current challenges. Applied Physics B: Lasers and Optics, 2022, 128, 72.	1.1	21
105	Multichannel light detectors and their use for CARS spectroscopy. Applied Optics, 1984, 23, 4083.	2.1	20
106	Diesel Spray Structure Investigation by Laser Diffraction and Sheet Illumination. , 0, , .		20
107	A robust and accurate algorithm of the β-pdf integration and its application to turbulent methane–air diffusion combustion in a gas turbine combustor simulator. International Journal of Thermal Sciences, 2002, 41, 763-772.	2.6	20
108	Characterization of few-layer graphene aerosols by laser-induced incandescence. Carbon, 2020, 167, 870-880.	5.4	20

#	Article	IF	CITATIONS
109	Flame Surface Fractal Characteristics in Premixed Turbulent Combustion at High Turbulence Intensities. AIAA Journal, 2007, 45, 2785-2789.	1.5	19
110	Some theoretical considerations in modeling laser-induced incandescence at low-pressures. Applied Physics B: Lasers and Optics, 2007, 87, 179-191.	1.1	19
111	The importance of international standards for the graphene community. Nature Reviews Physics, 2021, 3, 233-235.	11.9	19
112	Visualization and image analysis of droplet puffing and micro-explosion in spray-flame synthesis of iron oxide nanoparticles. Experiments in Fluids, 2022, 63, 1.	1.1	18
113	Optical properties of pulsed laser heated soot. Applied Physics B: Lasers and Optics, 2011, 104, 307-319.	1.1	17
114	Optimization of measurement angles for soot aggregate sizing by elastic light scattering, through design-of-experiment theory. Journal of Quantitative Spectroscopy and Radiative Transfer, 2012, 113, 355-365.	1.1	17
115	Spectrally resolved measurement of flame radiation to determine soot temperature and concentration. AIAA Journal, 2002, 40, 1789-1795.	1.5	17
116	The importance of thermal radiation transfer in laminar diffusion flames at normal and microgravity. Journal of Quantitative Spectroscopy and Radiative Transfer, 2011, 112, 1241-1249.	1.1	16
117	Evaluation of the absorption line blackbody distribution function of CO2 and H2O using the proper orthogonal decomposition and hyperbolic correlations. Journal of Quantitative Spectroscopy and Radiative Transfer, 2013, 128, 27-33.	1.1	16
118	Influence of rapid laser heating on the optical properties of in-flame soot. Applied Physics B: Lasers and Optics, 2015, 119, 621-642.	1.1	16
119	An improved CARS spectrometer for singleâ€shot measurements in turbulent combustion. Review of Scientific Instruments, 1992, 63, 5556-5564.	0.6	15
120	Application of Statistical Narrowband Model to Three-Dimensional Absorbing-Emitting-Scattered Media. Journal of Thermophysics and Heat Transfer, 1999, 13, 285-291.	0.9	15
121	Control of the structure and sooting characteristics of a coflow laminar methane/air diffusion flame using a central air jet: An experimental and numerical study. Proceedings of the Combustion Institute, 2011, 33, 1063-1070.	2.4	15
122	Demonstration of the CPMA-Electrometer System for Calibrating Black Carbon Particulate Mass Instruments. Aerosol Science and Technology, 2015, 49, 152-158.	1.5	15
123	A numerical study of laminar methane/air triple flames in two-dimensional mixing layers. International Journal of Thermal Sciences, 2006, 45, 586-594.	2.6	14
124	Effect of fuel composition on properties of particles emitted from a diesel–natural gas dual fuel engine. International Journal of Engine Research, 2021, 22, 77-87.	1.4	14
125	Closure between particulate matter concentrations measured ex situ by thermal–optical analysis and in situ by the CPMA–electrometer reference mass system. Aerosol Science and Technology, 2020, 54, 1293-1309.	1.5	13
126	Aircraft engine particulate matter emissions from sustainable aviation fuels: Results from ground-based measurements during the NASA/DLR campaign ECLIF2/ND-MAX. Fuel, 2022, 325, 124764.	3.4	13

#	Article	IF	CITATIONS
127	The structure of the dense core region in transient diesel sprays. Proceedings of the Combustion Institute, 1994, 25, 371-379.	0.3	12
128	Transient Particulate Matter Measurements from the Exhaust of a Direct Injection Spark Ignition Automobile. , 2001, , .		12
129	Evaluation of the laminar diffusion flamelet model in the calculation of an axisymmetric coflow laminar ethylene–air diffusion flame. Combustion and Flame, 2006, 144, 605-618.	2.8	12
130	Sequential signal detection for high dynamic range time-resolved laser-induced incandescence. Optics Express, 2017, 25, 2413.	1.7	12
131	Effective density and metals content of particle emissions generated by a diesel engine operating under different marine fuels. Journal of Aerosol Science, 2021, 151, 105651.	1.8	12
132	Systematic experimental comparison of particle filtration efficiency test methods for commercial respirators and face masks. Scientific Reports, 2021, 11, 21979.	1.6	12
133	Noise characteristics of single-shot broadband CARS signals. Applied Optics, 1987, 26, 4298.	2.1	11
134	Three-dimensional non-grey gas radiative transfer analyses using the statistical narrow-band model. International Journal of Thermal Sciences, 1998, 37, 759-768.	0.2	11
135	Effects of laser fluence non-uniformity on ambient-temperature soot measurements using the auto-compensating laser-induced incandescence technique. Applied Physics B: Lasers and Optics, 2016, 122, 1.	1.1	11
136	Development of a Sub-ppb Resolution Methane Sensor Using a GaSb-Based DFB Diode Laser near 3270 nm for Fugitive Emission Measurement. ACS Sensors, 2022, 7, 564-572.	4.0	11
137	A numerical investigation on NOX formation in counterflow n-heptane triple flames. International Journal of Thermal Sciences, 2007, 46, 936-943.	2.6	10
138	Numerical simulation aided relative optical density analysis of TEM images for soot morphology determination. Proceedings of the Combustion Institute, 2007, 31, 861-868.	2.4	10
139	Aircraft-engine particulate matter emissions from conventional and sustainable aviation fuel combustion: comparison of measurement techniques for mass, number, and size. Atmospheric Measurement Techniques, 2022, 15, 3223-3242.	1.2	10
140	Measurement of soot concentration and bulk fluid temperature and velocity using modulated laser-induced incandescence. Applied Physics B: Lasers and Optics, 2015, 119, 697-707.	1.1	9
141	Crumpled few-layer graphene: Connection between morphology and optical properties. Carbon, 2021, 182, 677-690.	5.4	9
142	Physical and chemical properties of black carbon and organic matter from different combustion and photochemical sources using aerodynamic aerosol classification. Atmospheric Chemistry and Physics, 2021, 21, 16161-16182.	1.9	9
143	Size-dependent mass absorption cross-section of soot particles from various sources. Carbon, 2022, 192, 438-451.	5.4	9

144 Flame Surface Density Measurements with PLIF in an SI Engine. , 1996, , .

8

	\sim	
	SMALLWOO	
UKLUI	JIVIALLVVOO	

#	Article	IF	CITATIONS
145	Ash-Decorated and Ash-Painted Soot from Residual and Distillate-Fuel Combustion in Four Marine Engines and One Aviation Engine. Environmental Science & Technology, 2021, 55, 6584-6593.	4.6	8
146	Multiphoton induced photoluminescence during time-resolved laser-induced incandescence experiments on silver and gold nanoparticles. Journal of Applied Physics, 2021, 129, .	1.1	8
147	Relationship between soot volume fraction and LII signal in AC-LII: effect of primary soot particle diameter polydispersity. Applied Physics B: Lasers and Optics, 2013, 112, 307-319.	1.1	7
148	Do Turbulent Premixed Flame Fronts in Spark-Ignition Engines Behave Like Passive Surfaces?. , 0, , .		6
149	Repeatability and intermediate precision of a mass concentration calibration system. Aerosol Science and Technology, 2019, 53, 701-711.	1.5	6
150	A numerical study on the effect of CO addition on extinction limits and NO _{<i>x</i>} formation in lean counterflow CH ₄ /air premixed flames. Combustion Theory and Modelling, 2007, 11, 741-753.	1.0	5
151	A Numerical Study on the Effect of Water Addition on NO Formation in Counterflow CH4/Air Premixed Flames. Journal of Engineering for Gas Turbines and Power, 2008, 130, .	0.5	5
152	An Improved Phenomenological Soot Formation Submodel for Three-Dimensional Diesel Engine Simulations: Extension to Agglomeration of Particles into Clusters. Journal of Engineering for Gas Turbines and Power, 2008, 130, .	0.5	5
153	Estimate of scattering truncation in the cavity attenuated phase shift PM _{SSA} monitor using radiative transfer theory. Aerosol Science and Technology, 2018, 52, 588-596.	1.5	5
154	The effect of preferential diffusion on soot formation in a laminar ethylene/air diffusion flame. Combustion Theory and Modelling, 2010, 15, 125-140.	1.0	4
155	Effect of recondensation of sublimed species on nanoparticle temperature evolution in time-resolved laser-induced incandescence. Applied Physics B: Lasers and Optics, 2015, 119, 607-620.	1.1	4
156	Response to <i>ACS Nano</i> Editorial "Standardizing Nanomaterials― ACS Nano, 2020, 14, 14255-14257.	7.3	4
157	An accurate efficient and flexible SNBCK-based unified band model for calculations of spectrally resolved and integrated quantities in participating media containing real-gases. , 2002, , .		4
158	Investigating renewable fuel combustion II: DNS of DME and nâ€heptane ignition in a turbulent nonâ€homogeneous flow with high dissipation. International Journal of Environmental Studies, 2007, 64, 419-432.	0.7	3
159	Effects of the Fractal Prefactor on the Optical Properties of Fractal Soot Aggregates. , 2009, , .		3
160	Effects of Detection Wavelengths on Soot Volume Fraction Measurements Using the Auto-Compensating LII Technique. Combustion Science and Technology, 2022, 194, 144-158.	1.2	3
161	Measurement of black carbon emissions from multiple engine and source types using laser-induced incandescence: sensitivity to laser fluence. Atmospheric Measurement Techniques, 2022, 15, 241-259.	1.2	3
162	Numerical Calculations of Heat Conduction Between Soot Aggregates and the Surrounding Gas in the Free-Molecular Regime Using the DSMC Method. , 2005, , 419.		2

#	Article	IF	CITATIONS
163	Numerical Study of Temperature and Incandescence Intensity of Nanosecond Pulsed-Laser Heated Soot Particles at High Pressures. , 2005, , 355.		2
164	Molecular Dynamics Simulations of Translational Thermal Accommodation Coefficients for Time-Resolved LII. , 2008, , .		2
165	A Numerical Investigation on Soot Formation From Laminar Diffusion Flames of Ethylene/Methane Mixture. , 2008, , .		2
166	THE IMPORTANCE OF THERMAL RADIATION TRANSFER IN LAMINAR DIFFUSION FLAMES AT NORMAL AND MICROGRAVITY. , 2010, , .		2
167	A CRITICAL EVALUATION OF THE THERMAL ACCOMMODATION COEFFICIENT OF SOOT DETERMINED BY THE LASER-INDUCED INCANDESCENCE TECHNIQUE. , 2006, , .		2
168	Effect of EGR on Heavy-Duty Diesel Engine Emissions Characterized With Laser-Induced Incandescence. , 2002, , .		2
169	Radiation Heat Transfer in SOFC Electrolytes. , 2005, , 183.		1
170	Influence of Pressure on Soot Formation in Laminar Diffusion Flames of Methane. , 2005, , .		1
171	A Numerical Investigation of NOx Formation in Counterflow CH4/H2/Air Diffusion Flames. , 2006, , .		1
172	Particulate Measurement Methods. , 2003, , 221-257.		1
173	Numerical Modeling of a Lifted Laminar Coflow Methane Diffusion Jet Flames Using Detailed Chemistry and Non-Grey Gas Radiation Models. , 2002, , 119.		0
174	Solution of Abel's Integral Equation Using Tikhonov Regularization. , 2005, , 301.		0
175	A Numerical Study on the Effect of Water Addition on NO Formation in Counterflow CH4/Air Premixed Flames. , 2005, , 383.		0
176	Experimental Investigation of Oxygen Addition to Fuel on Soot Formation in Laminar Coflow Diffusion Flames of Ethylene and Propane. , 2006, , 119.		0
177	Determining Aerosol Particle Size Distribution Using Time-Resolved Laser-Induced Incandescence. , 2006, , 405.		0
178	Measurement of Thermal Accommodation Coefficients Using Laser-Induced Incandescence. , 2007, , 477.		0
179	Investigating renewable fuel combustion I: comparative simulations of a diesel engine fuelled with nâ€e ₁₂ alkane and nâ€e ₁₈ fatty acidâ€derived liquidâ€property fuel. International Journal of Environmental Studies, 2007, 64, 401-418.	0.7	0

180 Structure of a Partially Premixed Iso-Octane/Air Turbulent V-Flame. , 0, , .

#	Article	IF	CITATIONS
181	Radiative Properties of Numerically Generated Fractal Soot Aggregates: The Importance of Configuration Averaging. , 2009, , .		0
182	Numerical Study of the Effects of Pressure and Gravitational Acceleration on Soot Formation in Laminar Axisymmetric Coflow Methane/Air Diffusion Flame. , 2009, , .		0
183	Optimum Angles for Multi-Angle Elastic Light Scattering Experiments. , 2011, , .		0
184	Numerical Study of Confined Laminar CH ₄ /Air Diffusion Flames Established in an Inverted Burner. Combustion Science and Technology, 2014, 186, 657-671.	1.2	0
185	A Numerical Study of the Influence of Hydrogen Addition on Soot Formation in a Laminar Counterflow Ethylene/Oxygen/Nitrogen Diffusion Flame. , 2004, , .		0
186	An Improved Soot Formation Model for 3-D Diesel Engine Simulations. , 2005, , .		0
187	A Numerical Study on a V-Shaped Laminar Stratified Flame. , 2005, , .		0
188	An Improved Phenomenological Soot Formation Sub-Model for 3-D Diesel Engine Simulations: Extension to Agglomeration of Particles Into Clusters. , 2006, , .		0
189	SOOT PARTICLE SIZING BY INVERSE ANALYSIS OF MULTIANGLE ELASTIC LIGHT SCATTERING. , 2010, , .		0
190	A Study of Isothermal Flow Past a Confined Bluff Body. , 1990, , .		0
191	A CRITERION FOR EVALUATION OF THE VALIDITY OF BLACK CARBON REFRACTIVE INDEX FROM		Ο